PHILOSOPHICAL TRANSACTIONS B

royalsocietypublishing.org/journal/rstb

Research

Cite this article: Huttenlocker AK, Shelton CD. 2020 Bone histology of varanopids (Synapsida) from Richards Spur, Oklahoma, sheds light on growth patterns and lifestyle in early terrestrial colonizers. *Phil. Trans. R. Soc. B* **375**: 20190142.
http://dx.doi.org/10.1098/rstb.2019.0142

Accepted: 30 August 2019

One contribution of 15 to a theme issue 'Vertebrate palaeophysiology'.

Subject Areas:
palaeontology

Keywords:
amniote, growth marks, skeletochronology, Permian, bone compactness

Author for correspondence:
Adam K. Huttenlocker
e-mail: ahuttenlocker@gmail.com

Bone histology of varanopids (Synapsida) from Richards Spur, Oklahoma, sheds light on growth patterns and lifestyle in early terrestrial colonizers

Adam K. Huttenlocker[1] and Christen D. Shelton[2]

[1]Department of Integrative Anatomical Sciences, University of Southern California, Los Angeles, CA 90033, USA
[2]Natural History Department, New Jersey State Museum, Trenton, NJ 08625-0530, USA

AKH, 0000-0002-7335-3208; CDS, 0000-0003-2689-2177

Varanopids were a group of small to medium-sized synapsids whose fossil record spans the Carboniferous through middle Permian. Although their phylogenetic relationships have received some interest in recent years, little is known about other aspects of their palaeobiology, including their skeletal growth, allometry and habitat preference. Here, we describe varanopid long bone histology based on a sample of well-preserved femora from the lower Permian Richards Spur fissure fill locality, Comanche County, Oklahoma, USA. The sample includes five femora from at least two varanopid taxa—*Mycterosaurus* and the large varanodontine *Varanops brevirostris*—and four additional mycterosaurine femora not diagnosed to genus. Prior work on femoral bone compactness provided a baseline to make lifestyle inferences and evaluate whether varanopids were ancestrally terrestrial. Moreover, the large availability of specimens spanning different sizes made possible an assessment of size-related ontogenetic histovariability. All specimens revealed moderately dense cortical bone tissues composed of sparsely vascularized parallel-fibred and lamellar bone with radially arranged rows of longitudinal canals (mostly simple), and many preserved regularly spaced growth marks (annuli and lines of arrested growth) as in modern varanids. We show that bone histology has the potential to explain how ballast was shed and the skeleton lightened for terrestrial mobility in ancestral synapsids and their basal amniote kin, as well as how adjustments in postnatal growth influenced the evolution of larger body sizes in the terrestrial frontier.

This article is part of the theme issue 'Vertebrate palaeophysiology'.

1. Introduction

The Synapsida represent one of the two major land-vertebrate clades that diverged from reptile-line amniotes during the late Carboniferous, *ca* 320 million years ago (Ma) [1–3]. Palaeontologists have long speculated about innovations in the life histories and reproductive physiology of these early amniotes, including how and when their ancestors developed extra-embryonic membranes and detached themselves from dependency on permanent water sources for reproduction, and how this novel ecology might have driven their skeletal biology. Prior work relied on anecdotal observations to address reproduction and ancestral life habitus in stem amniotes or 'reptiliomorphs' [4–6]. Laurin [7] later evaluated these hypotheses in a phylogenetic context, arguing that the earliest amniotes were larger than previously estimated (snout–vent length up to 24 cm and no less than 12 cm) and that their postnatal skeletal growth was most likely released from the constraint of small egg size. Evolutionary size increases apparently applied to the amniote stem, but not universally to early tetrapods.

While early amniotes and stem amniotes exhibited a variety of body sizes and ecologies by the Carboniferous–Permian transition, synapsid fossils in particular reveal patterns of increasing body length and myriad dietary ecologies [7,8],

THE ROYAL SOCIETY PUBLISHING

reflecting either a passive tendency to move away from their presumably small ancestral sizes or relaxation of prior ecophysiological constraints on size [9,10]. Turner & Tracy [11] emphasized the importance of postnatal body size, arguing that in some synapsids large size favoured terrestrial homeothermy (involuntary maintenance of a constant internal body temperature). This transition coincided with the eventual expansion of dryland-adapted faunas in seasonal environments of western Pangea *ca* 300 Ma, which covered even palaeotropical latitudes [12].

Importantly, whether the amniotic egg is optimized for terrestrial reproduction is tangential to whether the earliest amniotes were primarily terrestrial animals [13]. Ichnological (e.g. trackways) and palaeoenvironmental evidence provide tantalizing albeit circumstantial evidence, but the integration of comparative and functional training datasets in a rigorous phylogenetic framework has begun to offer robust models for 'retrodicting' the physiology and behaviours of extinct amniotes [14–16]. For example, bone compactness—the distribution of mineralized bone matrix in a cross-section—has been used to retrodict life habitus in some early synapsids, as well as other amniotes. In particular, Kriloff *et al*. [14] and Canoville & Laurin [15] showed evidence from the tibia and humerus, respectively, that extant amniotes bearing more tubular, less compact limb bone shafts tend toward terrestrial lifestyles, and some stem amniotes and basal synapsids also exhibited this condition. In particular, this challenged earlier notions that the synapsid *Ophiacodon* was a primarily aquatic ambush predator [17,18], although Canoville & Laurin [15] could not rule out that *Ophiacodon* was partially amphibious. More recently, Laurin & de Buffrénil [13] analysed femoral cross-sections from additional ophiacodontids, including *Clepsydrops*, corroborating that their limb bone compactness was best optimized for a terrestrial existence. Contemporary research suggests that the synapsid *Dimetrodon*, ophiacodontids, and their immediate ancestors included animals that were highly capable terrestrial predators with a capacity for multi-year growth to large body sizes while minimizing overall bone mass [13,19]. Nevertheless, despite Romer's [17] outdated views of ophiacodontid behaviour and phylogeny, the taxa studied to date do not necessarily reflect the ancestral state of Synapsida. Thus, while advances in palaeohistology have begun to address skeletal adaptation in Carboniferous–Permian synapsids with some statistical rigour, description of new material from key clades remains critical for improving the precision and confidence of our retrodictions.

Early investigations of synapsid bone histology were limited to a few well-represented taxa (e.g. *Dimetrodon*, *Edaphosaurus*) and isolated bones (e.g. [20,21]), prohibiting an in-depth understanding of histovariation within the group, especially in its basal-most members. The most prolific pioneering work was conducted by Enlow [22,23] and de Ricqlès [24–28], who broadly concluded that pelycosaur-grade synapsids exhibited more 'reptile-like' growth and only limited skeletal remodelling compared with the mammal-like Permo-Triassic therapsids. Renewed interest in synapsid palaeohistology in the past decade has revealed previously underappreciated histovariability in some groups, with limited sampling in the basal caseasaurs [29,30], varanopids [31], ophiacodontids [13,32], edaphosaurids [31,33] and sphenacodontids [31,34–36]. For example, the large carnivores *Ophiacodon*, *Sphenacodon* and *Dimetrodon* have shown evidence of rapid bone formation during early growth, in contrast to the caseasaurs and edaphosaurids. However, these are the only basal synapsid taxa to be investigated in a relatively complete ontogenetic series to date.

Of the major basal synapsids, the palaeobiology of Varanopidae remains poorly understood, largely owing to the rarity of their fossil remains. Varanopids represent a long-lived eupelycosaur clade that shared many superficial characteristics with extant monitor lizards, including long, slender limbs and sometimes recurved, ziphodont teeth [37], and survived from the late Carboniferous until the later part of the middle Permian [38]. A few varanopid taxa have been examined histologically, including the varanodontines *Varanops* [27,29,31] and *Watongia* [28,39], and a mycterosaurine from the lower Permian of Comanche County, Oklahoma [29,31]. Histologically, varanopid taxa show some degree of variation in tissue textures, vascularity, and growth zone formation. Moreover, the wide-open medulla of varanopid limb bones contrasts with some other early tetrapods, which typically exhibited a more pachyostotic medullary region, highly occluded by the spongiosa. This redistribution of bone mass may suggest evidence of more efficient terrestrial locomotion in varanopids [31].

Here, we present the first detailed descriptions of femoral microanatomy in Varanopidae, updated from the preliminary reports of Huttenlocker & Rega [31] and Shelton [29]. Huttenlocker & Rega [31] described briefly the limb bone histology of two varanopids they referred to *Varanops brevirostris* and a small mycterosaurine—likely *Mycterosaurus*—both from near Richards Spur, Oklahoma, USA. *Mycterosaurus* represents one of the most common vertebrates from this locality, second only to the basal eureptile *Captorhinus* [40]. For the present study, the sample of femora were combined with additional histological collections produced during Shelton's [29] survey of basal synapsid histology, and were analysed for bone compactness, tissue texture, vascularization, growth marks, and other important histological features. All material comes from the aforementioned lower Permian Richards Spur fissure fill Lagerstätte. The site represents an 'upland' assemblage dominated by amniotes and presumed terrestrial amphibians, with few anomalous aquatic elements [37,41,42]. Based on their excellent preservation and distinctive histological profile, we show a departure from the stem amniote condition—which was dominated by lamellar cortical bone that is highly compact—and reveal transitional motifs that instead began to resemble adults of more derived eupelycosaurs (e.g. *Ophiacodon*, *Dimetrodon*), as well as modern varanid analogues. Palaeohistological data offered here will contribute to a more robust hypothesis of skeletal adaptation in a key fossil clade near the synapsid–reptile dichotomy.

2. Material and methods

All materials described here come from a single fossil locality in Comanche County, Oklahoma, USA. The Dolese Brother's limestone quarry near Richards Spur preserves a lower Permian fissure fill deposit within an Ordovician limestone, whose fossils have been dated to approximately 289 to 286 Ma (Artinskian global stage) using speleothem U–Pb dating [42,43]. The most abundant synapsid remains from this locality belong to the varanopid *Mycterosaurus* cf. *M. longiceps* ([40]; '*Mycterosaurus* sp.' of [44] and [37]). Nine femora belonging to two taxa, *Mycterosaurus* and *Varanops*, were sampled for this study. Three femora referred conservatively to the genus *Mycterosaurus* were included: UWBM 89464, 89466, 98580 (figure 1*a–c*). Other small varanopid femora sampled here were not as well preserved or lacked key

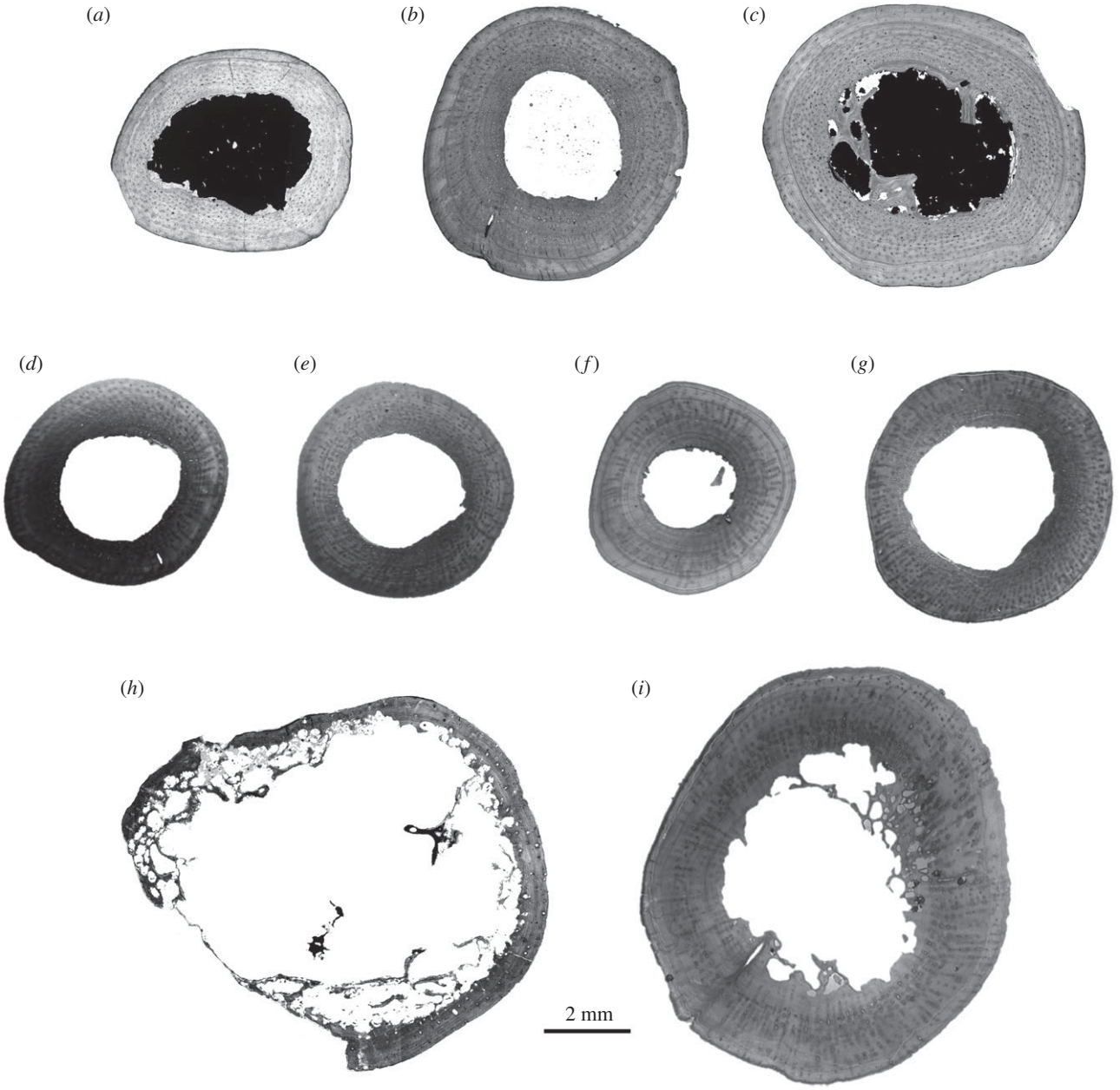

Figure 1. Sample of nine varanopid synapsid femora, sectioned at midshaft, from the Permian Richards Spur locality, Oklahoma, including *Mycterosaurus* (*a–c*), small mycterosaurine (*d–g*) and the varanodontine *Varanops brevirostris* (*h,i*). (*a*) *Mycterosaurus*, UWBM 89466; (*b*) *Mycterosaurus*, UWBM 98580; (*c*) *Mycterosaurus*, UWBM 89464; (*d*) mycterosaurine, OMNH 73750c; (*e*) mycterosaurine, OMNH 73354; (*f*) mycterosaurine, OMNH 73750b; (*g*) mycterosaurine, OMNH 73750a; (*h*) *Varanops*, UWBM 89463 (distal shaft cross-section); and (*i*) *Varanops*, OMNH 73758. All sections are shown to scale. Measurements are presented in table 1.

features owing to their small size, and are thus referred only to Mycterosaurinae/Varanopidae, but these most likely also represent small individuals of *Mycterosaurus*: OMNH 73750a, 73750b, 73750c, 73354 (figure 1*d–g*). A second varanopid assigned to the varanodontine *V. brevirostris* is also well known from the locality [44]. Two large femora assigned to *V. brevirostris* were thin-sectioned here: OMNH 73758, UWBM 89463 (figure 1*h,i*).

Sectioning and imaging protocols followed standard procedures for fossil bone outlined by Wilson *et al*. [45] and Lamm [46]. After photographing the specimens, each was embedded in a cold-mounting resin that was allowed to set overnight, then sectioned at the diaphysis in 1 mm wafers using a low-speed precision saw with a diamond blade. Transverse sections were cut from the middle diaphysis in most specimens, at about the level of the nutrient foramen, except in the *Varanops* UWBM 89463, which was sectioned at the distal shaft owing to its completeness. Longitudinal sections were also made for UWBM 98580. Wafers were glued onto frosted petrographic slides with an epoxy resin and then ground further to a thickness of approximately 100 µm using a mechanical grinder/polisher, then polished by hand to remove fine scratches using a polishing cloth. Thin-sections were imaged using normal, elliptical and circularly polarized light settings with a Leica DM 2700 microscope fitted with a motorized stage and digital image capture system.

In order to evaluate femoral compactness profiles for potential terrestrial adaptation, the digital scans of the cross-sections were converted to binary 8-bit images in Adobe Photoshop CC (Adobe Systems) and imported into the software Bone Profiler [47]. Bone Profiler estimates bone compactness (the relative area of a cross-section occupied by mineralized bone tissue) by calculating the proportion of bone area observed in 51 zones averaged across 60 radial sectors, and constructs a 'compactness profile' from the centroid to the periphery of the outer bone wall. Several parameters of the compactness profile can be used to describe the distribution of bone mass within a cross-section, some of which have been shown to correlate with lifestyle based on humeral and femoral profiles in a sample of extant amniotes [15,16]. Parameters discussed here include: cortico-diaphyseal index (CDI), the thickness of the cortex divided by

Table 1. Varanopid specimens sampled histologically and associated measurements. CDI, cortico-diaphyseal index [47]; Circ, midshaft circumference in mm; *K*, relative medullary diameter; *P*, relative position of inflection point; PF-LAM, parallel-fibred to lamellar bone transition (*sensu* [49]) with simple canals and/or osteons; *S*, slope of medulla–cortex transition zone; $Vasc_{dens}$, density of vascular canals per mm^2.

identification	no.	element	length (circ)	tissue-type	$Vasc_{dens}$	CDI	*K*	*P*	*S*
Mycterosaurus	UWBM 89466	femur	52 (16)	PF-LAM	56	0.468	0.51	0.53	0.02
Mycterosaurus	UWBM 89464	femur	65 (23)	PF-LAM	41	0.542	0.44	0.45	0.01
Mycterosaurus	UWBM 98580	femur	70 (24)	PF-LAM	100	0.518	0.49	0.48	0.05
Mycterosaurinae	OMNH 73750c	femur	49 (17)	PF-LAM	48	0.472	0.51	0.52	0.01
Mycterosaurinae	OMNH 73354	femur	50 (17)	PF-LAM	65	0.458	0.52	0.54	0.01
Mycterosaurinae	OMNH 73750b	femur	51 (18)	PF-LAM	70	0.587	0.42	0.41	0.02
Mycterosaurinae	OMNH 73750a	femur	57 (22)	PF-LAM	91	0.433	0.54	0.56	0.01
Varanops	UWBM 89463	femur	– (28)	PF-LAM	24	0.172	0.72	0.82	0.04
Varanops	OMNH 73758	femur	88 (37)	PF-LAM	49	0.472	0.58	0.53	0.04

the bone radius; *P*, the position of the inflection point between the less mineralized medulla and the more mineralized cortex; and *S*, the slope of the medulla–cortex transition zone. The relative medullary diameter, *K* [48], was also measured, as the ratio between the internal and external diameter of the bone. We predicted that, given the unique upland setting of the Richards Spur assemblage, the sampled varanopid femora should exhibit relatively low compactness and an open or unoccluded medulla reflective of a terrestrial lifestyle. For this purpose, we also compared limb compactness profiles in two sympatric eureptiles, *Captorhinus* and an indeterminate diapsid. Measurements are presented in table 1.

Histological descriptions were facilitated by the scanned photomicrographs at 50× and 100× total magnification under varied light settings. Elliptical and circular polarization were used to accurately identify fibre orientations and describe tissue texture, which can be somewhat diverse even in basal synapsid taxa [29,31]. The terminology and diagnosis of histotypes used here mainly follows the systems of de Margerie *et al*. [50] and McFarlin [49,51]. Tissue types and related histological features are abbreviated as follows: LAM, lamellar tissue; PF, parallel-fibred tissue; PF-LAM, parallel-fibred to lamellar bone transition (*sensu* [49, fig. 5.3]; PFO, parallel-fibred bone with primary osteons; and WB, woven-fibred tissue. Cyclic growth marks were also surveyed and described where noted, including annuli and/or lines of arrested growth (LAGs). Additional histometric measurements, including vascular density ($Vasc_{dens}$), were obtained by analysing the original photomicrographs in ImageJ v.1.47 [52]. Vascular density is defined here as the average number of canals observed per mm^2 (see protocol of [53]). In combination with tissue texture, vascular density and osteonal organization have been shown to reflect growth rate in extant amniotes [50,54], and are adopted here as proxies for relative growth in the varanopids. Vascular measurements are also reported in table 1.

In order to build a hypothesis of character histories—including ancestral bone compactness and vascularity—the data were combined with a published phylogenetic dataset that is here expanded from the study of Huttenlocker & Farmer [53]. Because an authoritative source of tetrapod divergence dates is lacking, branch lengths were approximated using median divergence dates from the Time Tree of Life project (http://www.timetree.org). Geological dates for fossil taxa were obtained from FossilWorks (http://www.fossilworks.org). The geological time-scale adopted here is based on the 2014 International Chronostratigraphic Chart circulated by the International Commission on Stratigraphy (updated from [55]). Zero-length branches were converted arbitrarily to a minimum of 1.0 Myr. The reference tree was built in Mesquite 1.0 [56] and phylogenetic character mapping was performed using the PDAP module [57]. Standardized residual contrasts for size (femoral circumference) and vascularity were also regressed in PDAP to test for correlated character evolution that might explain observed variations in cortical vascularity and tissue texture as they relate to body size.

3. Description of histological profiles in sampled femora

(a) *Mycterosaurus* (figures 1*a–c*, 2 and 6*a*)

The three femora sectioned here ranged from approximately 52–70 mm in length (16–24 mm in circumference) (table 1), thus falling in the size range of other *Mycterosaurus* fossils reported from the locality [40]. The femora are somewhat gracile, slender with a narrow shaft and proximal and distal ends. The intertrochanteric fossa is short with prominent anterior ridge nearly contacting the proximal articular surface, and the internal trochanter and adductor ridge are modestly developed. The smooth, black bone is generally well preserved with little damage or any evidence of recrystallization, presenting ideal optics for demonstrating discrete histological features (e.g. vasculature, growth marks) as well as the organization and texture of the original bone matrix. Minor portions of the bone, mainly internal cavities, are infilled with mud matrix and calcite, and have in places become pyritized (optically extinct areas in figures 1 and 2).

Despite their small, gracile appearance, the cortical walls of the femora are moderately thick and dense at the midshaft, approximately 1.5 to 2 mm or 21% of the cross-sectional diameter. This gives the gestalt of a highly compacted cortex. However, this is offset by an abrupt transition to a wide, open medullary (marrow) cavity with little to no cancellous bone. Coarse trabecular structures are present internally only closer to the proximal and distal diaphysis (near the metaphyses). At the midshaft, the deep portions of the cortex preserve dense primary bone tissue with little endosteal resorption and no evidence of compact-to-cancellous conversion in this area. In places, this smooth boundary is demarcated by endosteally deposited inner circumferential lamellae (icl; figure 2*d*). Given the large size of the medullary cavity, global compactness of the femoral midshaft was

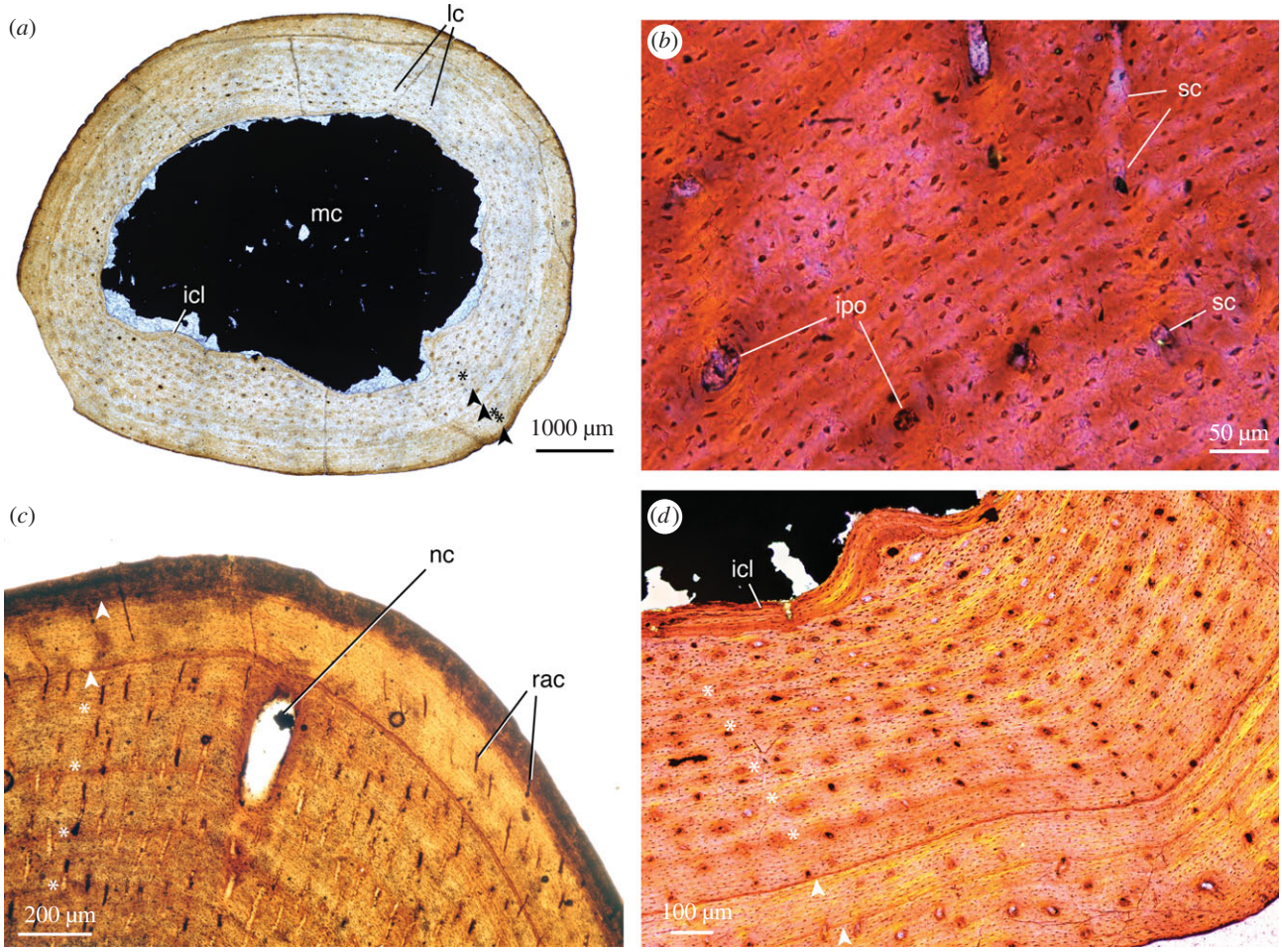

Figure 2. Detailed photomicrographs of mycterosaurine histology. (*a*) *Mycterosaurus*, UWBM 89466, femur midshaft at low magnification, normal (non-polarized) light; (*b*) same as '*a*,' midcortex viewed at high magnification, elliptical polarized light with quarter-wave retardation plate; (*c*) *Mycterosaurus*, UWBM 98580, femur midshaft, normal (non-polarized) light; (*d*) *Mycterosaurus*, UWBM 89464, femur midshaft viewed at high magnification, elliptical polarized light with quarter-wave retardation plate. Growth marks are present throughout the cortex in all sizes: asterisks indicate annuli, arrowheads indicate lines of arrested growth (LAGs). Abbreviations used in photographs of sections in this article: ec, erosion cavities; icl, inner circumferential lamellae; ipo, incipient primary osteons (*sensu* [36]); lam, lamellar bone; lc, longitudinal canals; lnv, non-vascular lamellar bone; mc, medullary (marrow) cavity; nc, nutrient canal; ocl, outer circumferential lamellae; pf, parallel-fibred tissue; pf-lam, parallel-fibred–lamellar transition; rac, radial canals; rc, reticular canals; sc, simple canals.

therefore low in all specimens (CDI, 0.468–0.542; *K*, 0.44–0.51), and showed no clear trend with increasing size.

The size of the medullary cavity limits our interpretation of the earliest growth phase, but subadult growth patterns can be generalized from all three specimens owing to the maintenance of primary bone and limited remodelling throughout the cortex. All femora show excellent preservation of growth marks bearing a naturally dark stain that makes them discernible under normal (non-polarized) light. Multiple zones of densely packed longitudinal vascular canals within a parallel-fibred to lamellar matrix are preserved in the inner cortex. The zones are delimited by faint annuli of denser bone (asterisks, figure 2) that are somewhat regularly spaced, recording a rhythm of lamellated, periosteal bone apposition. Some zones are followed by distinct lines of arrested growth (LAGs: arrowheads, figure 2) instead of annuli. However, there is no clear pattern in the relative distribution of annuli versus LAGs, whose formation may have been somewhat variable across individuals. The bone matrix becomes increasingly dense with fewer vascular spaces in the outermost cortex, particularly in larger individuals (UWBM 98580, 89464; figure 2*c*,*d*). The largest femur, UWBM 89464, includes at least one (and possibly a second) stark LAG in the outer one-third of the cortex (figure 2*d*), followed by poorly vascularized zones composed of mainly lamellar bone. Tissue changes likely represent a gradual decrease in growth rate, but the outer circumferential lamellae are not arranged into a distinct, avascular external fundamental system (EFS, [58]). The lack of a growth asymptote suggests instead that some capacity for skeletal growth was still possible up to the time of death, even in large specimens.

The organization of the vascular and lacunar spaces presents important ontogenetic and phylogenetic considerations. The vascular canals are predominantly simple, with most lacking concentric lamellae along their inner (endosteal) surfaces. Some areas preserve incipient primary osteons, showing the beginnings of concentric lamellation as described in the sphenacodont *Dimetrodon* [36], particularly within the deeper portions of the cortex representing earlier bone formation. The majority of outer canals, however, are simple canals. The canals are widely spaced ($Vasc_{dens}$, 41.6–100 canals per mm^2) and are oriented longitudinally, but are frequently arranged into radial rows. Some may bear slightly radial orientations, particularly within thicker growth zones or in thicker areas of the cross-section (figure 2*c*). The osteocyte lacunae similarly take on an orderly appearance, being predominantly lenticular in shape, their long-axes aligning with the surrounding lamellae. The sparse vasculature and orderly tissue texture, formed

predominantly by alternating patterns of PF-LAM, are consistent with an interpretation of prolonged, cyclic growth.

(b) Mycterosaurinae indet. (figure 1*d–g*)

The four additional mycterosaurine femora will be summarized together, noting that their histological profiles are nearly identical to that described above in *Mycterosaurus*. The slender femora, which range in size from 49 to 57 mm in length, have a circular midshaft cross-section with a moderately thick bone wall (CDI, 0.433–0.587; *K*, 0.42–0.54). Trabecular structures in the medulla are mostly absent at the midshaft level, as shown in *Mycterosaurus*.

In transverse section, it can be seen that lightly vascularized transitional PF-LAM prevails throughout the cortex. The vascular canals are mainly small, longitudinal canals that may be simple or osteonal. Thin radial canals, arrayed from the inner to outer cortex, also perfuse the cortex, forming a sunburst or 'bicycle wheel' pattern as observed in limb bones of other carnivorous eupelycosaurs [29,36]. The canals exhibit a relatively low density ($Vasc_{dens}$, 48–91 canals per mm^2). The bone matrix is speckled with densely packed osteocyte lacunae with flattened, lenticular shapes and aligned with the lamellae. The cortical bone contains, on average, a record of three to four growth marks visible in conventional light (not counting earlier growth marks that would have become obliterated by the expansion of the medullary cavity). Sharpey's fibres are not present. As in *Mycterosaurus*, inner circumferential lamellae are visible in polarized light around the medullary cavity. There is no EFS in the specimens.

(c) *Varanops brevirostris* (figures 1*h–i* and 3*a–c*)

The two sampled *Varanops* femora show broad similarities to *Mycterosaurus*, suggesting important family-level features of varanopid histology, but there are notable differences between the genera. The robust elements included a complete left femur sectioned at the midshaft (OMNH 73758), and a second partial left femur sectioned at the distal shaft (UWBM 89463). As expected, the well-preserved bone walls appear generally thinner closer to the metaphysis than at the midshaft, but both sections are proportionately thinner-walled than in the mycterosaurines. For example, the midshaft bone wall is of similar thickness to that in the mycterosaurines, being approximately 1.5 to 2 mm thick, despite the larger femoral diameter of *Varanops*. The relatively compact cortex transitions to coarse cancellous bone with prominent secondary trabecular structures (remodelled primary bone) and a relatively cavernous marrow space. Unlike the mycterosaurine samples, an inner circumferential layer was not established, and the endosteal lining of the medullary cavity was instead festooned by large erosion cavities carving into the cortical wall (figure 3*b*,*c*). Overall bone compactness was lower in *Varanops* than the majority of mycterosaurine femora described above, although values overlapped with some (CDI, 0.172–0.472; *K*, 0.58–0.72).

Growth rhythms are best recorded in the midshaft section of OMNH 73354, where a thicker wall of primary bone is preserved without as much internal erosion (figure 1*i*). There were at least five and as many as six growth marks (including both annuli and LAGs) visible in the specimen under normal light, although the innermost was largely obliterated by the expanding medullary cavity. The inner growth marks appear as annuli, whereas the outer three zones were punctuated by distinct LAGs that became more closely spaced peripherally

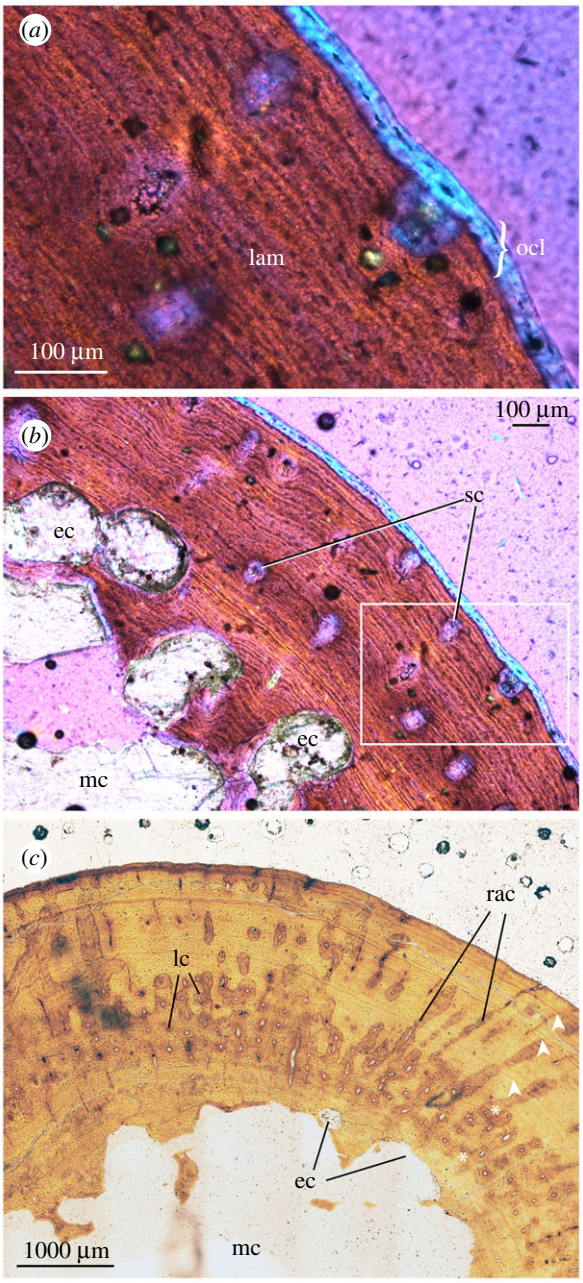

Figure 3. Detailed photomicrographs of *Varanops* histology. (*a*) *Varanops*, UWBM 89463, femur distal shaft at high magnification, elliptical polarized light with quarter-wave retardation plate; (*b*) same as (*a*) (inset), viewed at low magnification, elliptical polarized light with quarter-wave retardation plate; (*c*) *Varanops*, OMNH 73354, femur midshaft, normal (non-polarized) light. Abbreviations as in figure 2. (Online version in colour.)

(figure 3*c*). In UWBM 89463, there is an intriguing shell of avascular outer circumferential lamellae, about two or three lamellae thick (ocl, figure 3*a*), with fibre orientations apparently perpendicular to that of the underlying bone matrix. This switch in matrix organization is detectable on the basis of the elliptical polarization and reorientation of the long-axis of the osteocyte lacunae, which are considerably longer on the transverse plane in this zone.

The vascular motifs and tissue textures exhibited by *Varanops* were similar to those found in the mycterosaurine samples. The majority of the cortex was formed by alternating PF-LAM, with lamellar bone becoming more predominant toward the periphery. Primary osteons and simple canals were sparsely distributed throughout the highly lamellated

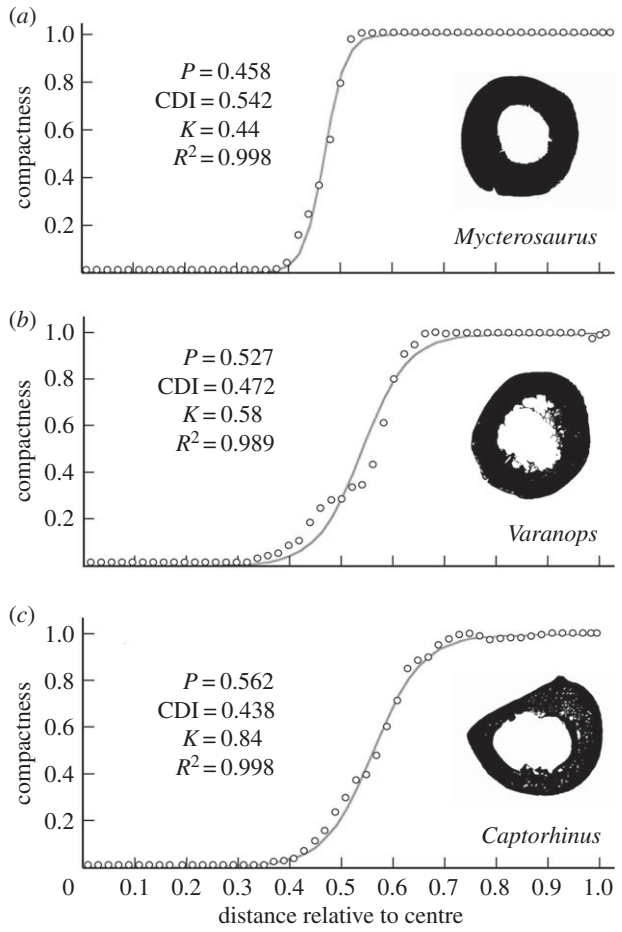

Figure 4. Femur midshaft compactness profiles of representative varanopid and *Captorhinus* specimens. (*a*) *Mycterosaurus*, UWBM 98580; (*b*) *Varanops*, OMNH 73758; (*c*) the eureptile *Captorhinus*, UMNH VP 25967. Values represent: *P*, position of the inflection point; CDI, cortico-diaphyseal index; and *K*, relative medullary diameter. Measurements for individual varanopids analysed in Bone Profiler [47] are listed in table 1.

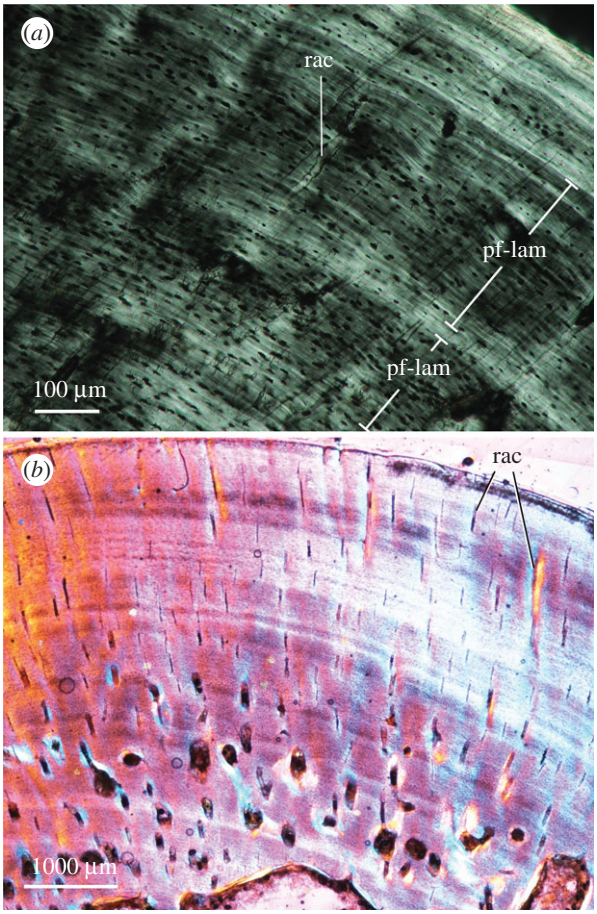

Figure 5. Exemplar photomicrographs of extant varanid analogues. (*a*), *Varanus niloticus*, MNHN FAOML-1996-69, femur midshaft, linear polarized light; (*b*), *Varanus komodoensis*, UWBM 8082, femur midshaft, elliptical polarized light with quarter-wave retardation plate. Abbreviations as in figure 2. (Online version in colour.)

bone matrix, their orientation being mainly longitudinal, but with a few radial canals in some locations forming a distinctive starburst or 'bicycle wheel' motif (figure 3*c*). Vascular density was low overall ($Vasc_{dens}$, 24–49 canals per mm^2). In UWBM 89463 (figure 3*a*,*b*), the cortex was dominated by lamellar bone with sparse simple canals having longitudinal orientations. The osteocyte lacunae are densely packed, lenticular in shape, and arranged into rows that parallel the sheet-like lamellae. Sharpey's fibres are present in localized areas, best visualized under polarized light.

4. Discussion of results

(a) Bone compactness and lifestyle inference in Richards Spur varanopids

In general, femur compactness profiles of Richards Spur varanopids reveal a relatively tubular cross-section, having a dense, moderately thickened cortex but with limited internal cancellous structure (figure 4). Cancellous trabeculae are more obvious in the *Varanops* sections than in mycterosaurines. The resulting 'hollow cylinder' structure is noteworthy given that many other basal amniotes, such as the eureptile *Captorhinus* (figure 4*c*), and stem amniotes preserve a more oval or teardrop cross-section, partly due to the hypertrophied adductor ridge that spans much of the femur length in the latter. The more cylindrical build in varanopids permits greater resistance to torsion and multidirectional bending [59,60], and possibly indicates a wider range of hindlimb motion in varanopids than in other early amniotes such as captorhinid eureptiles.

In terms of the circular distribution of mineralized bone matrix, the bone compactness parameters are consistent with a terrestrial life habitus in varanopids (as suggested for other eupelycosaurs; [13]). The perimedullary margin of mycterosaurine femora is smoothly finished by endosteally deposited inner circumferential lamellae, whereas that of *Varanops* is highly irregular. The relative medullary diameter is also more restricted in mycterosaurines (mean *K*, 0.49) than in *Varanops*, where the transition from the thin cortical wall to the medulla was more gradual (mean *K*, 0.65) (figure 4*a*,*b*). Nevertheless, only moderate levels of femoral compactness are observed in mycterosaurines (mean CDI, 0.496; mean *P*, 0.49) and especially in *Varanops* (mean CDI, 0.322; mean *P*, 0.67). Despite the difference in eccentricity mentioned above, these values are broadly similar to *Captorhinus*, also from the Richards Spur assemblage (figure 4*c*). These contrast, however, with published values for more aquatic taxa, where bone mass is distributed closer to the centroid (see [16]).

Germain & Laurin [18] originally argued for an aquatic lifestyle in the synapsid *Ophiacodon* owing to the compactness of

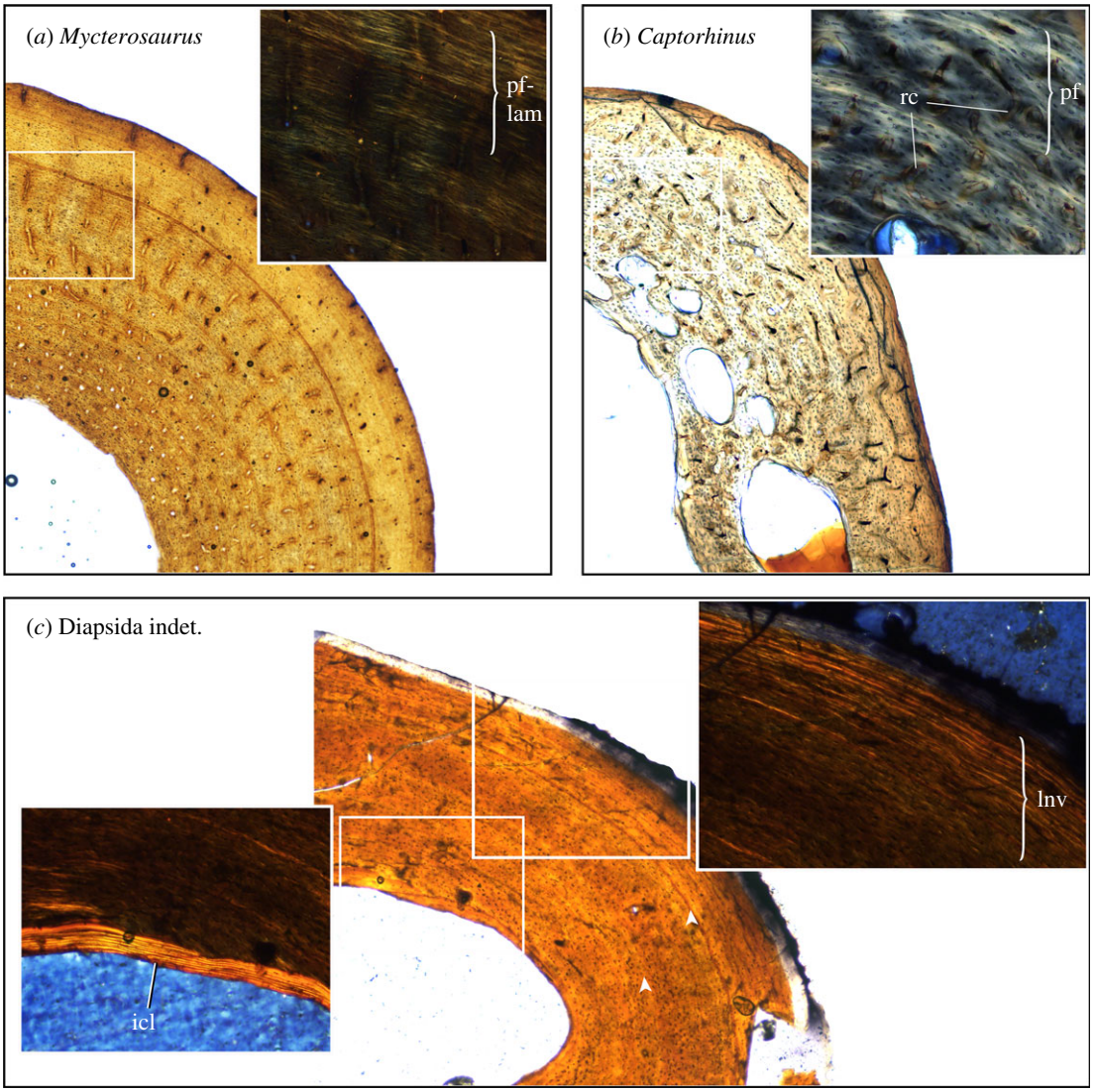

Figure 6. Comparison of tissue textures between varanopids and two sympatric eureptiles from Richards Spur, viewed in circularly polarized light (insets). (*a*) *Mycterosaurus* femur, UWBM 98580, shows cyclic PF-LAM with vascular canals arranged in radial rows; (*b*) the eureptile *Captorhinus* femur, UMNH VP 25968, shows disorganized bundles of PF with fewer growth marks and richly vascularized reticular bone; (*c*) Diapsida indet. (*Mycterosaurus longiceps* of [29, fig.3.3a]), OMNH 52543, humerus shows nonvascular lamellar bone that is interrupted by two LAGs (arrowheads). Abbreviations as in figure 2. (Online version in colour.)

the radius, but inferred this condition with low confidence given their meagre sample size. Improved predictive models based on extant amniote tibiae [14] and humeri [15] led the authors to revise this inference, showing instead that a terrestrial or only partially amphibious mode of life was more likely in *Dimetrodon* and *Ophiacodon*. Building on these studies, Laurin & de Buffrénil [13] included additional ophiacodontids, including femora of *Clepsydrops* and *Ophiacodon uniformis*, as well as the radius of *Ophiacodon retroversus* originally analysed by Germain & Laurin [18]. The authors concluded that ophiacodontids were primitively terrestrial, and the initial discrimination of *O. retroversus* as aquatic might have been based on variation in the proximo-distal location of the radial thin-section. Perhaps another reason for the incongruous results is the universally thick, compact radial cortex in synapsid quadrupeds compared with more proximal and hindlimb elements (e.g. [61]), making discrimination of a terrestrial or semiterrestrial animal less certain.

Overall, sampled synapsid limb bones suggest an ancestral condition that may have overlapped with values observed in semi- and fully terrestrial taxa, but their lifestyle discrimination based on femoral compactness tends toward terrestriality [13], broadly congruous with their functional anatomy [19] and palaeoenvironmental settings [12,37,41,42]. Any aquatic adaptations in the group were likely secondary. Significantly, *Varanops* is also notable for its larger size compared with mycterosaurines. A rough survey of other large-bodied basal synapsids shows that, as in *Varanops*, they too sometimes preserve cancellous structure within the medulla despite discriminating as terrestrial animals (e.g. see [36, figs 6,7; 32, figs. 1,6–14]). Thus, 'spongiosity' may also be size-related in basal synapsids, even though terrestrial mammal cursors show no such constraint by generally maintaining an open marrow cavity. Future investigation may identify a connection between bone size or robusticity and 'spongiosity' in basal synapsids, which could shed further light on locomotor changes during the basal synapsid-to-mammal transition. This constraint was presumably lifted during synapsid evolution in larger- (heavier-) limbed animals that were more erect and experienced more habitual bending but less frequent torsional loads as inferred in some therapsids [60].

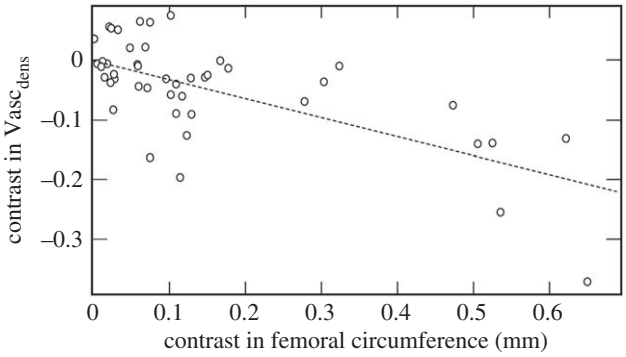

Figure 7. Standardized residual contrasts for femur circumference and vascular canal density ($Vasc_{dens}$) based on a phylogeny of tetrapods sampled histologically in a prior study (dataset updated from [53]; taxon sampling and tree shown in figure 8). Evolutionary increases in adult bone size were strongly correlated with fewer vascular canals per unit area (*N*, 45 contrasts; *r*, −0.764; $p < 0.001$) and thus a higher outer cortical bone density, despite having large canal diameters and high vascular area during the early growth phase. Data were log-transformed prior to analysis.

(b) Tissue texture, vascularity and evolution of growth patterns

In addition to lifestyle inferences, histological data from varanopids shed light on growth patterns in the basalmost synapsids and among early amniotes in general. Although recent years have seen a resurgence of studies on long bone growth in basal synapsids [13,29–32,36], prior sampling in varanopids was limited to two zeugopodial elements of *Varanops* (tentatively interpreted as a radius and fibula) [27]; an unsourced element belonging to the large varanodontine *Watongia* [28,39], and a handful of mycterosaurine and *Varanops* elements from Richards Spur which were described only briefly [31]. Our inspection reveals modest vascularization, formed mostly by simple canals and some incipient primary osteons, in an alternating PF-LAM matrix spanning multiple growth zones. Growth marks are abundant and suggest multi-year growth to moderate-to-large sizes (snout–vent length >12 cm) as in other large, predatory eupelycosaurs (e.g. *Dimetrodon*; [36]). Although their tissues are not as strongly lamellated or avascular as in most modern reptiles of similar size (e.g. iguanians; [62]), the samples bear striking resemblance to varanids (figure 5). Despite a range of growth strategies among varanid species [63], many larger varanids exhibit moderate cortical vascularity—mainly simple canals in longitudinal and radial orientations, with osteonal canals located in deeper regions—within an alternating PF-LAM matrix that becomes increasingly lamellar toward the periphery of the bone [54].

From a palaeoecological perspective, the diverse assemblage of Richards Spur also offers a window into the growth rhythms of Permian amniotes living at approximately palaeoequatorial latitudes, and, by extension, potential environmental impacts on their life histories. Histological data have been applied widely to other palaeoecological systems, including the Permian-aged Briar Creek assemblage [64] and the Beaufort Group assemblages of the Karoo Basin [65], as well as dinosaur assemblages of Inner Mongolia [66] and the Hell Creek Formation in Montana [67], to name a few. Peabody [68] offered the first survey of cyclic growth mark formation in Richards Spur vertebrates, recognizing at least two or three zones in different skeletal elements attributed to *Captorhinus*. He concluded that cyclic growth mark formation likely indicated seasonal climatic variations in western Pangea, despite the palaeotropical position of the locality during Permian times. New data from the varanopids sampled here are congruent with this hypothesis. Nevertheless, noteworthy histovariation is apparent among amniotes from this assemblage, supporting that some histological features are influenced by additional historical (phylogenetic) and niche-specific factors (diet, foraging behaviour) [69]. For example, *Captorhinus* has been suggested to record fewer skeletal growth marks than contemporary synapsids and diadectomorphs [70], an observation that is confirmed by our sectioning of additional comparative specimens from the Richards Spur assemblage (figure 6*b*). Other small eureptiles (figure 6*c*) may show strong incremental lamellar tissues with poor to no vascularization, as in iguanians [62]. The apparent histological diversity at the base of Amniota reinforces arguments that some histological traits carry an important phylogenetic signal (e.g. [15,69]), and suggests that phylogenetic comparative approaches are most appropriate to establish ancestral life-history patterns in Amniota.

The incorporation of primary vascular canals within the mineral matrix is somewhat variable in early amniotes and stem amniotes, but most crown amniotes that have been analysed in a phylogenetic context preserve moderate vasculature that permits inference of relative bone growth rate and vascular supply [71,72] (figures 7 and 8). In general, rapidly deposited bone incorporates a rich vascular supply, which becomes progressively less vascularized as growth slows nearing maturity [50,54]. Vascular density is modest in the varanopid femora sampled here, with slightly greater vascularization in the mycterosaurines than in the larger-bodied *Varanops* (*Mycterosaurus*: $Vasc_{dens}$ 74 canals per mm^2; *Varanops*: $Vasc_{dens}$ 36 canals per mm^2). Notably, larger tetrapods in our phylogenetic sample typically showed less vascular density than in their small-bodied relatives (Pearson's *r*, −0.764; $p < 0.001$) (figure 7), as highlighted by the apparent disparity between mycterosaurine and *Varanops* femora. This might suggest that selection for larger adult body size in some basal amniotes was driven initially by a capacity for prolonged, cyclic (and not necessarily accelerated) skeletal growth. However, some eupelycosaurs like *Ophiacodon* may have bucked this trend by further accelerating their subadult growth rates [32]. Optimization of histological traits on a phylogeny of early tetrapods suggests that the terrestrial (or semi-terrestrial) ancestors of amniotes were small to moderate-sized animals with modest skeletal growth rates and primary cortical tissues dominated by lamellar bone. Unlike eupelycosaurs, however, this tissue-type incorporated little to no primary vasculature and was highly lamellated, as seen in microsaurs, diadectomorphs, caseids, parareptiles and early diapsids, resembling the familiar cortical bone tissues of extant small to mid-sized lizards (e.g. iguanians). Among early amniotes, non-lamellar tissues (as in woven-fibred bone or incipient fibrolamellar bone; e.g. [32]) were encountered frequently only in the carnivorous lineages leading to therapsids and archosauromorphs (figure 8*a*), showing associated stepwise increases in their cortical vascularization (figure 8*b*). Systemic non-lamellar tissues were apparently rare to absent in the herbivorous caseids and edaphosaurids. [29], although woven-fibred tissues were localized in the tubercles of *Edaphosaurus* [33].

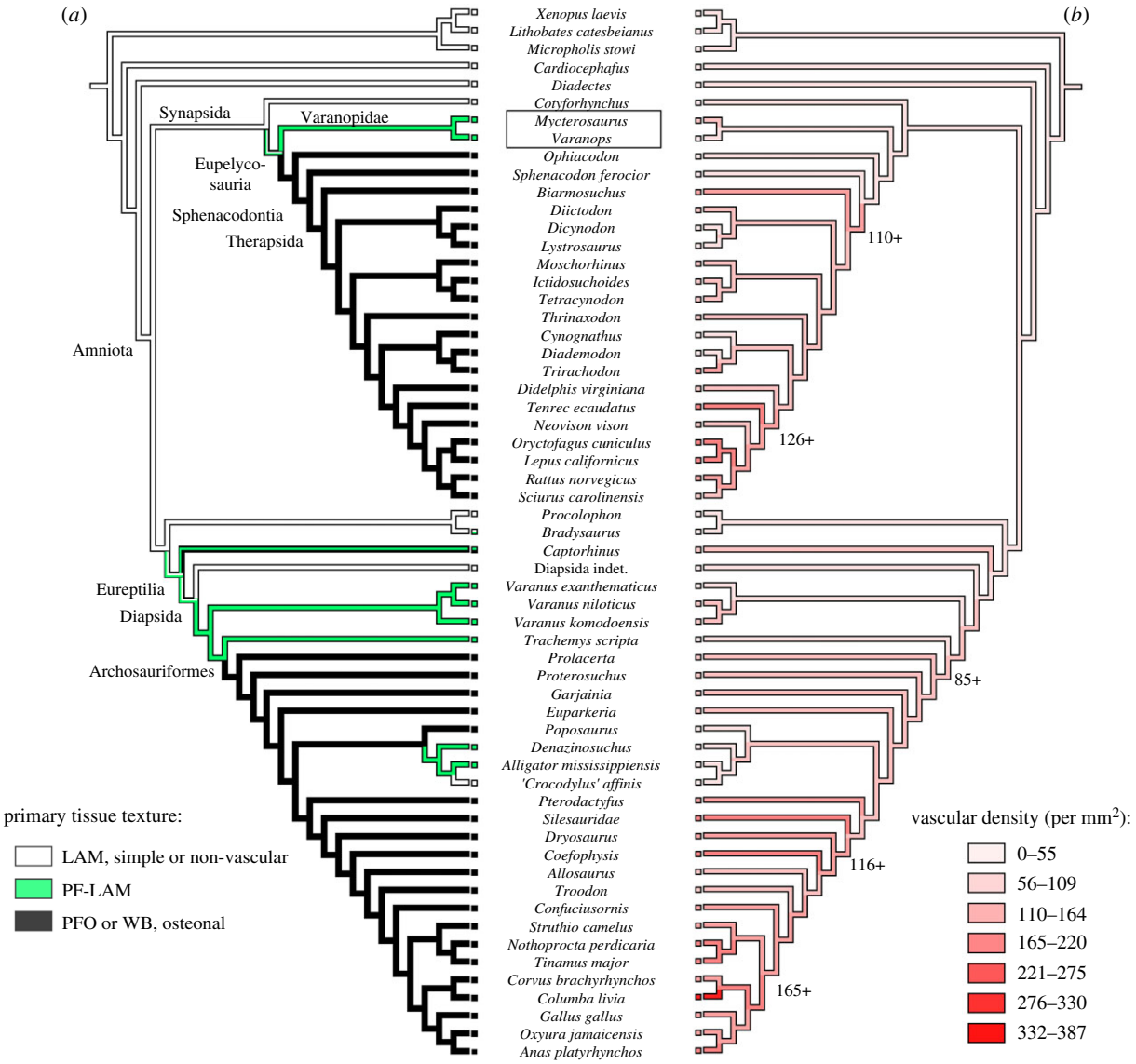

Figure 8. Evolution of bone tissue texture and cortical vasculature in synapsids and other early amniotes (see table 8). (*a*) Phylogenetic distribution and hypothesized character changes in tissue texture based on three categorical states: lamellar primary bone, parallel-fibred to lamellar transition, and non-lamellar, osteonal primary tissues, including PFO and woven-fibred bone. (*b*) Ancestral state reconstructions of vascular density ($Vasc_{dens}$) in early amniotes. Phylogenetic character mapping was performed using the PDAP module ([57] in Mesquite 1.0 [56]). LAM, lamellar primary bone; PF-LAM, parallel-fibred to lamellar transition; PFO, parallel-fibred bone with primary osteons; WB, woven-fibred bone. (Online version in colour.)

5. Conclusion

Histological data are consistent with recently accepted notions of synapsid palaeobiology, including their ancestral life histories, habitat preferences, and locomotor behaviour. Varanopid synapsids and their close relatives were likely capable terrestrial locomotors. Their cortical bone tissues provide evidence of continuous growth and internal bone resorption with low compactness, suggesting versatile limb mobility and strength, while also demonstrating multi-year growth to moderate-to-large body sizes. Their bone physiology mimicked that of extant varanid lizards, a group that includes active foragers capable of moderately sustained exercise and high aerobic scope [53], making them an uncanny modern analogue. More generally, optimization of histological traits on our reference phylogeny indicates that other basal amniotes and stem amniotes were typified by poorly vascularized bone dominated by lamellar-zonal tissues. Notable exceptions included the basal eureptile *Captorhinus*, which formed more vascular, disorganized bony tissues than similar-sized sympatric amniotes, likely reflective of its more rapid growth and/or shorter longevity. Varanopids also contrast in recording a pattern of vascular PF-LAM that broadly resembles adults of other carnivorous eupelycosaurs (e.g. *Ophiacodon*, *Sphenacodon*). These intriguing outliers highlight an underappreciated histological diversity during the early radiation of Amniota, even among species from the same assemblage.

Data accessibility. Data are available from the corresponding author (A.K.H.) by request.

Authors' contributions. A.K.H. and C.D.S. analysed the data, prepared figures and wrote the paper.

Competing interests. We declare we have no competing interests.

Funding. A.K.H. was supported by the National Science Foundation DEB-1209018 and DBI-1309040; C.D.S. was supported by DFG grant no. SA 469/34-1 and the University of Bonn.

Acknowledgements. We thank W. May for donating specimens for thin-sectioning. We also thank the repositories that accepted the resulting histology collections: C. Sidor and the University of Washington Burke Museum (UWBM), Seattle; R. Cifelli and the Sam Noble Oklahoma Museum of Natural History (OMNH), Norman; and R. Irmis and C. Levitt-Bussian and the Natural History Museum of Utah (UMNH), Salt Lake City. We thank J. Gardner and E.-T. Lamm

for access to additional fossil samples in the collection of Museum of the Rockies (MOR), Bozeman, and S. Echols, DVM, DABVP for providing bird tissue samples analysed for figure 8. For their support and insightful discussions, we also thank our collaborators J. Botha, C. Farmer, M. Sander and K. Stein. V. de Buffrénil is thanked for access to comparative material, including the extant varanid analogue *V. niloticus* shown in figure 5 (FAOML, UN Food and Agriculture Organization).

Appendix A

Table 2. List of taxa and specimens analysed for phylogenetic comparative analysis in figure 8. This sample is expanded from Huttenlocker & Farmer [53].

taxon	specimen/voucher no.	element	ref.
Temnospondyli			
Micropholis stowi	NMQR 3621; UCMP 78395b	humerus	[53]
Stem amniotes			
Cardiocephalus	OMNH 56886	femur	[73,74]
Diadectes	FMNH UR2514	femur	new
Reptilia (Sauropsida)			
Allosaurus	UUVP 2656; UUVP 3694	femur	[75]
Bradysaurus	SAM-PK-9137, 9165, 5127, 12057 12129, 9355	femur	[76]
Captorhinus sp.	UMNH VP 25964; UMNH VP 25966; UMNH VP 259 67; UMNH VP 25968	femur	[53], new
Coelophysis	UCMP 129618	femur	[77]
Confuciusornis	MOR 1063	femur	[77]
'Crocodylus' affinis	UWBM 89252; UWBM 88113	femur	[53]
Denazinosuchus	UMNH VP 16733	femur	new
Diapsida indet.	OMNH 52543	humerus	new
Dryosaurus	CM 1949	femur	[78]
Euparkeria capensis	SAM-PK-K10548; SAM-PK-K10010	femur	[79]
Garjainia madiba	BP/1/6232; BP/1/7217; BP/1/7219	femur	[80]
Poposaurus gracilis	YPM 57100	femur	[53]
Procolophon	NMQR 3944b; 3555b	femur	[81]
Prolacerta broomi	NMQR 3763	humerus	[53,79]
Proterosuchus fergusi	SAM-PK-K11208; SAM-PK-K140	femur	[79]
Pterodactylus	CM 11430	femur	[77]
Silesauridae	NHCC LB54; NHCC LB79	femur	[5,82]
Troodon	MOR 748	femur	[77]
Synapsida			
Biarmosuchus tener	PIN/401.1.1.T	humerus	[27]
Bienotherium yunnanense	YPM 13-I	femur	[24]
Cynognathus crateronotus	NMQR 3019; SAM-PK-6235	femur	[83]
Diademodon tetragonus	UCMZ T493; UCMZ T495; UCMZ T503	femur	[83]
Dicynodon	SAM-PK-5576	femur	[84]
Diictodon feliceps	SAM-PK-K5035; SAM-PK-K5282; SAM-PK-10174; SAM-PK-11099	femur	[84]
Ictidosuchoides longiceps	SAM-PK-K8659; SAM-PK-K10423	femur	[85]
Lystrosaurus	NMQR 835a	femur	[84]
Moschorhinus kitchingi	NMQR 3939; NMQR 3351; NMQR 3684	femur	[61,85]
Mycterosaurus	UWBM 89464; UWBM 89466; UWBM 98580	femur	[53]
Sphenacodon ferocior	UCMP 34209; UCMP 83628	femur	[31]
Tetracynodon darti	UCMP 78395; UCMP 78396	femur	[85]

(*Continued*.)

Table 2. (*Continued.*)

taxon	specimen/voucher no.	element	ref.
Thrinaxodon liorhinus	SAM-PK-1395; SAM-PK-K8004	femur	[86]
Trirachodon berryi	SAM-PK-5881	femur	[87]
Varanops brevirostris	OMNH 73758; UWBM 89463	femur	new

Institutional abbreviations: BP, Evolutionary Studies Institute (former Bernard Price Institute collection), Johannesburg; CM, Carnegie Museum of Natural History, Pittsburgh; MOR, Museum of the Rockies, Bozeman; NHCC, National Heritage Conservation Commission, Lusaka; NMQR, National Museum, Bloemfontein; OMNH, Sam Noble Oklahoma Museum of Natural History, Norman; PIN, Paleontological Institute, Moscow; SAM, Iziko South African Museum, Cape Town; UCMP, University of California Museum of Paleontology, Berkeley; UCMZ, University Museum of Zoology, Cambridge, UK; UMNH/UUVP, Natural History Museum of Utah, Salt Lake City; UWBM, University of Washington Burke Museum of Natural History and Culture, Seattle; YPM, Yale Peabody Museum, New Haven.

References

1. Gauthier J, Kluge AG, Rowe T. 1988 Amniote phylogeny and the importance of fossils. *Cladistics* **4**, 105–209. (doi:10.1111/j.1096-0031.1988.tb00514.x)
2. Gauthier JA. 1994 The diversification of the amniotes. *Short Courses Paleontol.* **7**, 129–159. (doi:10.1017/S247526300000129X)
3. Angielczyk KD. 2009 Dimetrodon is not a dinosaur: using tree thinking to understand the ancient relatives of mammals and their evolution. *Evol. Educ. Outreach* **2**, 257. (doi:10.1007/s12052-009-0117-4)
4. Romer AS. 1957 Origin of the amniote egg. *Scient. Monthly* **85**, 57–63.
5. Carroll RL. 1970 Quantitative aspects of the amphibian-reptilian transition. *Forma Functio* **3**, 165–178.
6. Carroll RL. 1991. The origin of reptiles. In *Origins of the higher groups of tetrapods: controversy and consensus* (eds H-P Schultze, L Trueb), pp. 331–353. Ithaca, NY: Comstock Publishing Associates.
7. Laurin M. 2004 The evolution of body size, Cope's rule and the origin of amniotes. *Syst. Biol.* **53**, 594–622. (doi:10.1080/10635150490445706)
8. Reisz RR, Fröbisch J. 2014 The oldest caseid synapsid from the Late Pennsylvanian of Kansas, and the evolution of herbivory in terrestrial vertebrates. *PLoS ONE* **9**, e94518. (doi:10.1371/journal.pone.0094518)
9. Stanley SM. 1973 An explanation for Cope's rule. *Evolution* **27**, 1–26. (doi:10.1111/j.1558-5646.1973.tb05912.x)
10. McShea DW. 1994 Mechanisms of large-scale evolutionary trends. *Evolution* **48**, 1747–1763. (doi:10.1111/j.1558-5646.1994.tb02211.x)
11. Turner JS, Tracy CR. 1986 Body size, homeothermy and the control of heat exchange in mammal-like reptiles. In *The ecology and biology of mammal-like reptiles* (eds N Hotton, PD MacLean, J Roth, EC Roth), pp. 185–194. Washington, DC: Smithsonian Institution Press.
12. Pardo JD, Small BJ, Milner AR, Huttenlocker AK. 2019 Carboniferous–Permian climate change constrained early land vertebrate radiations. *Nat. Ecol. Evol.* **3**, 200. (doi:10.1038/s41559-018-0776-z)
13. Laurin M, de Buffrénil V. 2016 Microstructural features of the femur in early ophiacodontids: a reappraisal of ancestral habitat use and lifestyle of amniotes. *C. R. Palevol* **15**, 115–127. (doi:10.1016/j.crpv.2015.01.001)
14. Kriloff A, Germain D, Canoville A, Vincent P, Sache M, Laurin M. 2008 Evolution of bone microanatomy of the tetrapod tibia and its use in palaeobiological inference. *J. Evol. Biol.* **21**, 807–826. (doi:10.1111/j.1420-9101.2008.01512.x)
15. Canoville A, Laurin M. 2010 Evolution of humeral microanatomy and lifestyle in amniotes, and some comments on palaeobiological inferences. *Biol. J. Linn. Soc.* **100**, 384–406. (doi:10.1111/j.1095-8312.2010.01431.x)
16. Quemeneur S, De Buffrenil V, Laurin M. 2013 Microanatomy of the amniote femur and inference of lifestyle in limbed vertebrates. *Biol. J. Linn. Soc.* **109**, 644–655. (doi:10.1111/bij.12066)
17. Romer AS. 1961 A large ophiacodont pelycosaur from the Pennsylvanian of the Pittsburgh region. *Bull. Mus. Comp. Zool.* **144**, 1–7.
18. Germain D, Laurin M. 2005 Microanatomy of the radius and lifestyle in amniotes (Vertebrata, Tetrapoda). *Zool. Scr.* **34**, 335–350. (doi:10.1111/j.1463-6409.2005.00198.x)
19. Felice RN, Angielczyk KD. 2014 Was *Ophiacodon* (Synapsida, Eupelycosauria) a swimmer? A test using vertebral dimensions. In *Early evolutionary history of the Synapsida* (eds C Kammerer, K Angielczyk, J Fröbisch), pp. 25–51. Dordrecht, The Netherlands: Springer.
20. Moodie RL. 1923 *Paleopathology. An introduction to the study of ancient evidences of disease*. Urbana, IL: University of Illinois Press.
21. Gross W. 1934 [The types of bone microstructure in the fossil stegocephalians and reptiles]. *Z. Anat. Entwickl.* **103**, 731–764. [In German.] (doi:10.1007/BF02118752)
22. Enlow DH, Brown SO. 1957 A comparative histological study of fossil and recent bone tissues. Part II. *Texas J. Sci.* **9**, 136–214.
23. Enlow DH. 1969 The bone of reptiles. In *Biology of the Reptilia volume 1: morphology A* (eds C Gans, A Bellairs, T Parsons), pp. 45–80. London, UK: Academic Press.
24. de Ricqlès, A. 1969 [Palaeohistological study of the long bones of some tetrapods, II: some observations on the long bone structure of some theriodonts]. *Ann. Paléontol. Vertébrés* **55**, 1–52. [In French.]
25. de Ricqlès A. 1972 [Palaeohistological study of the long bones of some tetrapods, III: titanosuchians, dinocephalians and dicynodonts]. *Ann. Paléontol. Vertébrés* **58**, 17–60. [In French.]
26. de Ricqlès A. 1974 Evolution of endothermy: histological evidence. *Evol. Theory* **1**, 51–80.
27. de Ricqlès A. 1974 Paleohistological research on the long bones of tetrapods IV: eotheriodonts and pelycosaurs. In *Ann. Paléontol.* **60**, 3–39.
28. de Ricqlès A. 1976 On bone histology of fossil and living reptiles, with comments on its functional and evolutionary significance. *Morphol. Biol. Reptiles* **3**, 123–149.
29. Shelton CD. 2015 Origins of Endothermy in the mammalian lineage. PhD dissertation, Universitäts und Landesbibliothek Bonn.
30. Lambertz M, Shelton CD, Spindler F, Perry SF. 2016 A caseian point for the evolution of a diaphragm homologue among the earliest synapsids. *Ann. N. Y. Acad. Sci.* **1385**, 3–20. (doi:10.1111/nyas.13264)
31. Huttenlocker AK, Rega E. 2012 The paleobiology and bone microstructure of pelycosaurian-grade synapsids. In *The forerunners of mammals: radiation, histology and biology* (ed. A Chinsamy-Turan), pp. 90–119. Bloomington, IN: Indiana University Press.
32. Shelton CD, Sander PM. 2017 Long bone histology of *Ophiacodon* reveals the geologically earliest occurrence of fibrolamellar bone in the mammalian stem lineage. *C. R. Palevol.* **16**, 397–424. (doi:10.1016/j.crpv.2017.02.002)
33. Huttenlocker AK, Mazierski D, Reisz R. 2011 Comparative osteohistology of hyperelongate neural spines in the Edaphosauridae (Amniota: Synapsida).

Palaeontology **54**, 573–590. (doi:10.1111/j.1475-4983.2011.01047.x)

34. Huttenlocker AK, Rega E, Sumida S. 2010 Comparative anatomy and osteohistology of hyperelongate neural spines in the sphenacodontids *Sphenacodon* and *Dimetrodon* (Amniota: Synapsida). *J. Morphol.* **271**, 1407–1421. (doi:10.1002/jmor.10876)
35. Rega EA, Noriega K, Sumida SS, Huttenlocker A, Lee A, Kennedy B. 2012 Healed fractures in the neural spines of an associated skeleton of *Dimetrodon*: implications for dorsal sail morphology and function. *Fieldiana Life Earth Sci.* **2012**, 104–111. (doi:10.3158/2158-5520-5.1.104)
36. Shelton CD, Sander PM, Stein K, Winkelhorst H. 2013 Long bone histology indicates sympatric species of *Dimetrodon* (Lower Permian, Sphenacodontidae). *Earth Environ. Sci. Trans. R. Soc. Edinb.* **103**, 217–236. (doi:10.1017/S175569101300025X)
37. Evans DC, Maddin HC, Reisz RR. 2009 A re-evaluation of sphenacodontid synapsid material from the Lower Permian fissure fills near Richards Spur, Oklahoma. *Palaeontology* **52**, 219–227. (doi:10.1111/j.1475-4983.2008.00837.x)
38. Modesto SP, Smith RM, Campione NE, Reisz RR. 2011 The last "pelycosaur": a varanopid synapsid from the *Pristerognathus* Assemblage Zone, Middle Permian of South Africa. *Naturwissenschaften* **98**, 1027–1034. (doi:10.1007/s00114-011-0856-2)
39. Bennett AA, Ruben JA. 1986 The metabolic and thermoregulatory status of therapsids. In *The ecology and biology of mammal-like reptiles* (eds N Hotton, PD MacLean, JJ Rothand, EC Roth), pp. 207–218. Washington, DC: Smithsonian Institution Press.
40. Reisz RR, Wilson H, Scott D. 1997 Varanopseid synapsid skeletal elements from Richards Spur, a Lower Permian fissure fill near Fort Sill, Oklahoma. *Oklahoma Geol. Notes* **57**, 160–170. (doi:10.1111/j.1475-4983.2008.00837.x)
41. Olson EC. 1991 An eryopid (Amphibia: Labyrinthodontia) from the Fort Sill fissures, Lower Permian, Oklahoma. *J. Vertebr. Paleontol.* **11**, 130–132. (doi:10.1080/02724634.1991.10011379)
42. MacDougall MJ, Tabor NJ, Woodhead J, Daoust AR, Reisz RR. 2017 The unique preservational environment of the Early Permian (Cisuralian) fossiliferous cave deposits of the Richards Spur locality, Oklahoma. *Palaeogeogr. Palaeoclimatol. Palaeoecol.* **475**, 1–11. (doi:10.1016/j.palaeo.2017.02.019)
43. Woodhead J, Reisz R, Fox D, Drysdale R, Hellstrom J, Maas R, Cheng H, Edwards RL. 2010 Speleothem climate records from deep time? Exploring the potential with an example from the Permian. *Geology* **38**, 455–458. (doi:10.1130/G30354.1)
44. Maddin HC, Evans DC, Reisz RR. 2006 An Early Permian varanodontine varanopid (Synapsida: Eupelycosauria) from the Richards Spur locality, Oklahoma. *J. Vertebr. Paleontol.* **26**, 957–966. (doi:10.1671/0272-4634(2006)26[957:aepvvs]2.0.co;2)
45. Wilson JW, Leiggi P, May P. 1994 Histological techniques. *Vertebr. Paleontol. Tech.* **1**, 205–234.
46. Lamm E-T. 2013 Preparation and sectioning of specimens. In *Bone histology of fossil tetrapods: advancing methods, analysis, and interpretation* (eds K Padian and E-T Lamm), pp. 55–160. Berkeley, CA: University of California Press.
47. Girondot M, Laurin M. 2003 Bone profiler: a tool to quantify, model, and statistically compare bone-section compactness profiles. *J. Vertebr. Paleontol.* **23**, 458–461. (doi:10.1671/0272-4634(2003)023[0458:BPATTQ]2.0.CO;2)
48. Currey JD, Alexander RM. 1985 The thickness of the walls of tubular bones. *J. Zool.* **206**, 453–468. (doi:10.1111/j.1469-7998.1985.tb03551.x)
49. McFarlin SC. 2006 Ontogenetic variation in long bone microstructure in catarrhines and its significance for life history research. PhD dissertation, City University of New York.
50. de Margerie E, Cubo J, Castanet J. 2002 Bone typology and growth rate: testing and quantifying 'Amprino's rule'in the mallard (*Anas platyrhynchos*). *C. R. Biol.* **325**, 221–230. (doi:10.1016/S1631-0691(02)01429-4)
51. McFarlin SC, Terranova CJ, Zihlman AL, Bromage TG. 2016 Primary bone microanatomy records developmental aspects of life history in catarrhine primates. *J. Hum. Evol.* **92**, 60–79. (doi:10.1016/j.jhevol.2015.12.004)
52. Rasband WS. 1997–2015. *ImageJ*. Bethesda, MD: U.S. National Institutes of Health. See http://imagej.nih.gov/ij/.
53. Huttenlocker AK, Farmer CG. 2017 Bone microvasculature tracks red blood cell size diminution in Triassic mammal and dinosaur forerunners. *Curr. Biol.* **27**, 48–54. (doi:10.1016/j.cub.2016.10.012)
54. Buffrénil V de, Houssaye A, Böhme W. 2008 Bone vascular supply in monitor lizards (Squamata: Varanidae): influence of size, growth, and phylogeny. *J. Morphol.* **269**, 533–543. (doi:10.1002/jmor.10604)
55. Gradstein FM, Ogg JG, Schmitz M, Ogg G. 2012 *The geologic time scale 2012*. Oxford, UK: Elsevier.
56. Maddison WP, Maddison DR. 2014 *Mesquite: a modular system for evolutionary analysis. V. 1.0*. See http://www.mesquiteproject.org.
57. Midford PE, Garland T, Maddison WP. 2011 *PDAP: PDTREE module for Mesquite (version 1.16)*. See http://mesquiteproject.org/pdap_mesquite/index.html.
58. Cormack DH. 1987 *Ham's histology*, 9th edn, p. 732. New York, NY: Lippincott.
59. Blob RW. 2000 Interspecific scaling of the hindlimb skeleton in lizards, crocodilians, felids and canids: does limb bone shape correlate with limb posture? *J. Zool.* **250**, 507–531. (doi:10.1111/j.1469-7998.2000.tb00793.x)
60. Blob RW. 2001 Evolution of hindlimb posture in nonmammalian therapsids: biomechanical tests of paleontological hypotheses. *Paleobiology* **27**, 14–38. (doi:10.1666/0094-8373(2001)027<0014:EOHPIN>2.0.CO;2)
61. Huttenlocker AK, Botha-Brink J. 2013 Body size and growth patterns in the therocephalian *Moschorhinus kitchingi* (Therapsida: Eutheriodontia) before and after the end-Permian extinction in South Africa. *Paleobiology* **39**, 253–277. (doi:10.1666/12020)
62. Hugi J, Sánchez-Villagra MR. 2012 Life history and skeletal adaptations in the Galapagos marine iguana (*Amblyrhynchus cristatus*) as reconstructed with bone histological data—a comparative study of iguanines. *J. Herpetol.* **46**, 312–324. (doi:10.1670/11-071)
63. Buffrénil V, Ineich I, Böhme W. 2005 Comparative data on epiphyseal development in the family Varanidae. *J. Herpetol.* **39**, 328–336. (doi:10.1670/0022-1511(2005)039[0328:CDOEDI]2.0.CO;2)
64. Konietzko-Meier D, Shelton CD, Sander PM. 2016 The discrepancy between morphological and microanatomical patterns of anamniotic stegocephalian postcrania from the Early Permian Briar Creek Bonebed (Texas). *C. R. Palevol* **15**, 103–114. (doi:10.1016/j.crpv.2015.06.005)
65. Botha-Brink J, Codron D, Huttenlocker AK, Angielczyk KD, Ruta M. 2016 Breeding young as a survival strategy during Earth's greatest mass extinction. *Scient. Rep.* **6**, 24053. (doi:10.1038/srep24053)
66. Varricchio DJ, Sereno PC, Xijin Z, Lin T, Wilson JA, Lyon GH. 2008 Mud-trapped herd captures evidence of distinctive dinosaur sociality. *Acta Palaeontol. Pol.* **53**, 567–579. (doi:10.4202/app.2008.0402)
67. Horner JR, Goodwin MB, Myhrvold N. 2011 Dinosaur census reveals abundant *Tyrannosaurus* and rare ontogenetic stages in the Upper Cretaceous Hell Creek Formation (Maastrichtian), Montana, USA. *PLoS ONE* **6**, e16574. (doi:10.1371/journal.pone.0016574)
68. Peabody FE. 1961 Annual growth zones in living and fossil vertebrates. *J. Morphol.* **108**, 11–62. (doi:10.1002/jmor.1051080103)
69. Cubo J, Ponton F, Laurin M, De Margerie ED, Castanet J. 2005 Phylogenetic signal in bone microstructure of sauropsids. *Syst. Biol.* **54**, 562–574. (doi:10.1080/10635150591003461)
70. Warren JW. 1963 Growth zones in the skeleton of recent and fossil vertebrates. PhD dissertation, University of California Los Angeles.
71. Cubo J, Le Roy N, Martinez-Maza C, Montes L. 2012 Paleohistological estimation of bone growth rate in extinct archosaurs. *Paleobiology* **38**, 335–349. (doi:10.1666/08093.1)
72. Legendre LJ, Segalen L, Cubo J. 2013 Evidence for high bone growth rate in *Euparkeria* obtained using a new paleohistological inference model for the humerus. *J. Vertebr. Paleontol.* **33**, 1343–1350. (doi:10.1080/02724634.2013.780060)
73. Ricqlès A. 1981 [Palaeohistological study of the long bones of some tetrapods, VI: stegocephalians]. *Ann. Paléontol.* **67**, 141–160. [In French.]
74. Organ CL, Canoville A, Reisz RR, Laurin M. 2011 Paleogenomic data suggest mammal-like genome size in the ancestral amniote and derived large

genome size in amphibians. *J. Evol. Biol.* **24**, 372–380. (doi:10.1111/j.1420-9101.2010.02176.x)

75. Bybee PJ, Lee AH, Lamm ET. 2006 Sizing the Jurassic theropod dinosaur *Allosaurus*: assessing growth strategy and evolution of ontogenetic scaling of limbs. *J. Morphol.* **267**, 347–359. (doi:10.1002/jmor.10406)
76. Canoville A, Chinsamy A. 2017 Bone microstructure of pareiasaurs (Parareptilia) from the Karoo Basin, South Africa: implications for growth strategies and lifestyle habits. *Anat. Rec.* **300**, 1039–1066. (doi:10.1002/ar.23534)
77. Padian K, Horner JR, De Ricqlès A. 2004 Growth in small dinosaurs and pterosaurs: the evolution of archosaurian growth strategies. *J. Vertebr. Paleontol.* **24**, 555–571. (doi:10.1671/0272-4634(2004)024[0555:GISDAP]2.0.CO;2)
78. Horner JR, de Ricqlès A, Padian K, Scheetz RD. 2009 Comparative long bone histology and growth of the 'hypsilophodontid' dinosaurs *Orodromeus makelai*, *Dryosaurus altus*, and *Tenontosaurus tillettii* (Ornithischia: Euornithopoda). *J. Vertebr. Paleontol.* **29**, 734–747. (doi:10.1671/039.029.0312)
79. Botha-Brink J, Smith RMH. 2011 Osteohistology of the Triassic archosauromorphs *Prolacerta*, *Proterosuchus*, *Euparkeria*, and *Erythrosuchus* from the Karoo Basin of South Africa. *J. Vertebr. Paleontol.* **31**, 1238–1254. (doi:10.1080/02724634.2011.621797)
80. Gower DJ, Hancox PJ, Botha-Brink J, Sennikov AG, Butler RJ. 2014 A new species of *Garjainia* Ochev, 1958 (Diapsida: Archosauriformes: Erythrosuchidae) from the Early Triassic of South Africa. *PLoS ONE* **9**, e111154. (doi:10.1371/journal.pone.0111154)
81. Botha-Brink J, Smith RMH. 2012 Palaeobiology of Triassic procolophonids, inferred from bone microstructure. *C. R. Palevol.* **11**, 419–433. (doi:10.1016/j.crpv.2012.03.002)
82. Peecook BR, Steyer JS, Tabor NJ, Smith RM. 2017 Updated geology and vertebrate paleontology of the Triassic Ntawere Formation of northeastern Zambia, with special emphasis on the archosauromorphs. *J. Vertebr. Paleontol.* **37**(Suppl. 1), 8–38. (doi:10.1080/02724634.2017.1410484)
83. Botha J, Chinsamy A. 2001 Growth patterns deduced from the bone histology of the cynodonts *Diademodon* and *Cynognathus*. *J. Vertebr. Paleontol.* **20**, 705–711. (doi:10.1671/0272-4634(2000)020[0705:GPDFTB]2.0.CO;2)
84. Botha-Brink J, Angielczyk KD. 2010 Do extraordinarily high growth rates in Permo-Triassic dicynodonts (Therapsida, Anomodontia) explain their success before and after the end-Permian extinction? *Zool. J. Linn. Soc.* **160**, 341–365. (doi:10.1111/j.1096-3642.2009.00601.x)
85. Huttenlocker AK, Botha-Brink J. 2014 Bone microstructure and the evolution of growth patterns in Permo-Triassic therocephalians (Amniota, Therapsida) of South Africa. *PeerJ* **2**, e325. (doi:10.7717/peerj.325)
86. Botha J, Chinsamy A. 2005 Growth patterns of *Thrinaxodon liorhinus*, a non-mammalian cynodont from the Lower Triassic of South Africa. *Palaeontology* **48**, 385–394. (doi:10.1111/j.1475-4983.2005.00447.x)
87. Botha J, Chinsamy A. 2004 Growth and life habits of the Triassic cynodont *Trirachodon*, inferred from bone histology. *Acta Palaeontol. Pol.* **49**, 619–627.